A Cytomeglaoviral Protein Reveales a Dual Role for STAT2 in IFN-g Signaling and Antiviral Responses

Zimmermann, Albert; Trilling, Mirko; Wagner, Markus; Wilborn, Manuel; Bubić, Ivan; Jonjić, Stipan; Koszinowski, Ulrich; Hengel, Hartmut

A cytomegaloviral protein reveals a dual role for STAT2 in IFN-γ signaling and antiviral responses

Albert Zimmermann,[1] Mirko Trilling,[2] Markus Wagner,[3] Manuel Wilborn,[2] Ivan Bubic,[4] Stipan Jonjic,[4] Ulrich Koszinowski,[3] and Hartmut Hengel[1]

[1]Institut für Virologie, Heinrich-Heine-Universität Düsseldorf, 40225 Düsseldorf, Germany
[2]Division of Viral Infections, Robert Koch Institute, 13353 Berlin, Germany
[3]Department of Virology, Max von Pettenkofer Institute, 81377 Munich, Germany
[4]Department of Histology and Embryology, Faculty of Medicine, University of Rijeka, 51000 Rijeka, Croatia

A mouse cytomegalovirus (MCMV) gene conferring interferon (IFN) resistance was identified. This gene, *M27*, encodes a 79-kD protein that selectively binds and down-regulates for signal transducer and activator of transcription (STAT)-2, but it has no effect on STAT1 activation and signaling. The absence of pM27 conferred MCMV susceptibility to type I IFNs (α/β), but it had a much more dramatic effect on type II IFNs (γ) in vitro and in vivo. A comparative analysis of *M27*$^+$ and *M27*$^-$ MCMV revealed that the antiviral efficiency of IFN-γ was partially dependent on the synergistic action of type I IFNs that required STAT2. Moreover, STAT2 was directly activated by IFN-γ. This effect required IFN receptor expression and was independent of type I IFNs. IFN-γ induced increasing levels of tyrosine-phosphorylated STAT2 in *M27*$^-$ MCMV-infected cells that were essential for the antiviral potency of IFN-γ. pM27 represents a new strategy for simultaneous evasions from types I and II IFNs, and it documents an unknown biological significance for STAT2 in antiviral IFN-γ responses.

CORRESPONDENCE
Hartmut Hengel:
hartmut.hengel@
uni-duesseldorf.de

Abbreviations used: BAC, bacterial artificial chromosome; EMSA, electrophoretic mobility shift assay; GAS, γ-activated sequence; HA, hemagglutinin; HCMV, human CMV; IFNAR, IFN-α/β receptor; IFNGR, IFN-γ receptor; IRF, IFN response factor; ISGF3, IFN-stimulated gene factor 3; ISRE, IFN-stimulated response element; MCMV, mouse CMV; MEF, mouse embryonal fibroblast; PAA, phosphonoacetic acid; p.i., postinfection; SG, salivary gland; VV, vaccinia virus.

IFNs represent a major line of defense against viruses connecting innate and adaptive immunity. IFNs are classified into two distinct types: type I (α/β) and type II (γ). Type I IFNs are synthesized in direct response to an infection with a virus. IFN-α is encoded by a multigene family and is predominantly synthesized by leukocytes. In contrast, the product of the IFN-β gene is produced by most cell types, in particular by fibroblasts. IFN-γ is produced by activated T lymphocytes and NK cells in response to the recognition of virus-infected cells. The binding of IFN-α/β and IFN-γ to their cognate transmembrane receptors initiates distinct JAK-STAT–dependent signaling pathways (1, 2). The IFN α/β receptor (IFNAR) is composed of two subunits, IFNAR1 and IFNAR2. Upon ligand binding, receptor-associated TYK2 and JAK1 are activated and phosphorylate STAT2, which allows for the recruitment of STAT1 (3). Phosphorylated STAT1/STAT2 heterodimers are translocated to the nucleus and associate with the DNA-binding protein p48 to form the heterotrimeric IFN-stimulated gene factor 3 (ISGF3) complex, which binds to IFN-stimulated response element (ISRE) sequences of IFN-α/β–inducible genes (1, 3). IFN-γ receptors (IFNGRs) consist of IFNGR1 and IFNGR2, which are associated with JAK1 and JAK2, respectively (4). IFNGR triggering results in the formation of paired binding sites for STAT1. STAT1 homodimers translocate to the nucleus where they bind to γ-activated sequence (GAS) elements to activate transcription of IFN-γ–inducible genes. Although functional similarities between types I and II IFNs exist, the systems are not redundant with respect to the induction of specific genes and the control of certain virus infections.

CMVs constitute prototypes of the β-herpesviruses; human CMV (HCMV) and mouse CMV (MCMV) share a similar pathobiology and have collinear genomes. Cellular immunity and IFNs play prominent roles in CMV immune control (5–7). Specifically, IFN-γ is essential for the control of MCMV replication in the salivary glands (SGs) and the effector

M. Wagner's present address is Department of Pathology, Harvard Medical School, Boston, MA 02115.

function of $CD8^+$ T cells in vivo (5, 8). CMV genes affecting host immune functions increase the available time window for replication and facilitate virus shedding (9). The failure of infected cells to respond to both types of IFNs suggested that CMVs disrupt IFN receptor (IFNR) signaling by unknown gene functions (8, 10-12). We report on the identification and characterization of the first cytomegaloviral IFN response antagonist. To search for genes that disrupt IFN signaling, we pursued a systematic approach by constructing IFN-responsive, ISRE-reporting cell lines suitable for subsequent phenotypic screening with an MCMV Tn*Max*16-transposon insertion library. The discovered gene, *M27*, encoding a 79-kD protein, proved to be an inhibitor of both IFNAR- and IFNGR-mediated responses. The viral inhibitor down-regulated STAT2 exclusively, whereas STAT1-dependent functions remained unaffected. The dramatically increased susceptibility of ΔM27-MCMV replication to IFN-γ was dependent on IFN-β secretion, IFNAR signaling, and STAT2 activation; this demonstrated a synergistic action of type I IFNs with IFN-γ. In addition, STAT2 was found to be directly activated by IFN-γ in the absence of type I IFN responses. The findings document a direct, as well as an indirect, augmentation of IFNGR responses via STAT2 as a prerequisite for efficient antiviral gene expression in response to IFN-γ.

RESULTS

Identification of MCMV *M27* as a candidate gene affecting ISRE-dependent gene expression

To monitor viral functions affecting IFN-inducible transcription throughout the CMV replication cycle, we generated a reporter cell line expressing the luciferase gene under the control of an ISRE-dependent promoter. The 3T3-ISRE-luc cells responded to IFN-α in a dose-dependent manner over a range of 3–4 $\log_{10}$ steps of IFN concentration. After infection, the IFN-α–induced, ISRE-dependent luciferase activity continuously declined and was abolished 36 h p.i. (Fig. 1 A). This effect required MCMV gene expression because UV-inactivated MCMV was not capable of mediating this inhibition. In the presence of the CMV polymerase inhibitor phosphonoacetic acid (PAA), we observed a substantial inhibition of the IFN-α response, which indicated that MCMV E gene expression was required to block the IFN-α response. To identify the MCMV gene products responsible for this inhibition, we used a forward genetic procedure based on a random, single Tn insertion mutagenesis of the MCMV genome cloned as a bacterial artificial chromosome BAC (13). 3T3-ISRE-luc cells were infected with a large panel of reconstituted Tn*Max*16 containing MCMV BAC mutants and tested for an IFN-α–induced luciferase expression. Although the bulk of MCMV mutants were able to suppress the IFN-α–stimulated luciferase expression, three independent mutants failed to suppress the response. The Tn*Max*16 insertion site in all three mutants was mapped to the *M27* gene, which is dispensable for replication in vitro but plays an important role in growth and virulence in mice (14).

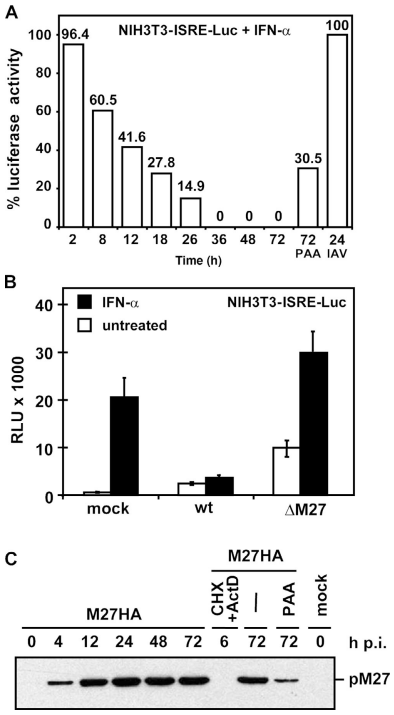

Figure 1. Inhibition of IFN-α–dependent luciferase induction by MCMV *M27*. (A) 3T3-ISRE-luc cells were infected with 10 PFU/cell MCMV-WT strain Smith and stimulated with 500 U/ml IFN-α for 5 h at the indicated time points p.i. Results were expressed as the percentage of luciferase activity in comparison with uninfected cells. The influence of viral gene expression was studied by the analysis of luciferase activity in the presence of PAA, which inhibits the expression of viral late gene expression, and by the analysis of UV-inactivated virus (IAV). (B) 3T3-ISRE-luc cells were infected with MCMV-WT, ΔM27-MCMV, or M27rev (10 PFU/cell each) and stimulated with 500 U/ml IFN-α for 5 h at 8 h (mock) or 29 h (MCMV-WT and ΔM27-MCMV) p.i. Luciferase activity was determined luminometrically as relative light units (RLU). Each value represents the mean ± SD from three independent experiments. (C) Expression kinetics of the M27 protein. MEFs were infected with 10 PFU/cell M27HA, and cell lysates were prepared at the indicated time points. Equivalent amounts of lysate were subjected to SDS-PAGE and then immunoblotted using anti-HA antibodies. The selective synthesis of MCMV IE proteins was achieved by infecting cells in the presence of 50 μg/ml of cycloheximide, which was then replaced by 5 μg/ml of actinomycin for a further 2 h. 250 μg/ml PAA was used to inhibit late phase gene expression.

We constructed a targeted mutant with a complete deletion of *M27* (ΔM27-MCMV) and a revertant virus (M27rev) in which the *M27* open reading frame was reinserted into the ΔM27-MCMV genome. In contrast to ΔM27-MCMV, the MCMV-WT and M27rev almost completely inhibited the IFN-α–induced ISRE response at 29 h p.i. (Fig. 1 B). An MCMV mutant expressing a hemagglutinin (HA)-tagged M27 protein (M27-HA) was constructed to determine the kinetics of M27 protein expression. The 79-kD M27 protein

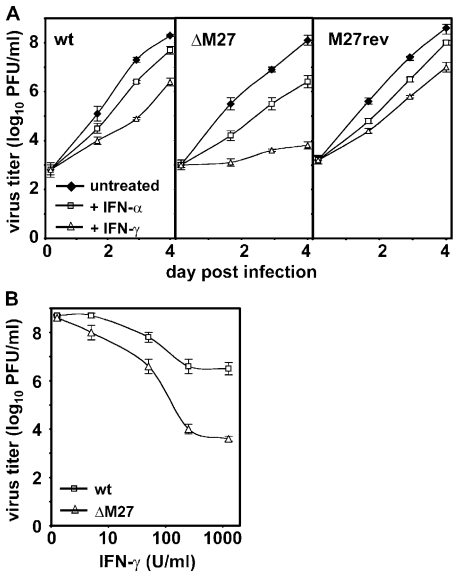

Figure 2. Inhibition of ΔM27-MCMV replication by IFN-α and IFN-γ. (A) Primary C57BL/6-MEFs were infected with MCMV-WT, ΔM27-MCMV, and M27rev (0.01 PFU/cell each). Titers of infectious virus were determined by a standard plaque assay. Growth curves were obtained after 48 h of preincubation of cells without IFN, 500 U/ml IFN-α, or 500 U/ml IFN-γ. (B) C57BL/6-MEFs were treated with graded concentrations of IFN-γ and infected as in A with MCMV-WT and ΔM27-MCMV (0.01 PFU/cell each). Viral titers obtained at 96 h p.i. were shown in relation to doses of IFN-γ.

(pM27) was detected 4 h p.i. and reached a maximal abundance at 24 h p.i. pM27 was not recovered under conditions of selective IE gene expression (Fig. 1 C). The viral polymerase inhibitor PAA decreased pM27 synthesis, indicating a typical early–late pattern of MCMV gene expression compatible with the time course of the MCMV-induced inhibition of ISRE-dependent transcription.

M27 confers resistance of MCMV replication against type I and type II IFNs

To prove that the candidate gene *M27* is causally related to IFN-induced cellular functions, a multistep replication analysis was performed. Primary C57BL/6 mouse embryonal fibroblasts (MEFs) pretreated with IFN-α and IFN-γ for 48 h before infection revealed a 5- and a 50-fold decrease, respectively, of MCMV-WT replication by 96 h p.i. (Fig. 2 A), confirming earlier results that demonstrated the moderate effect of IFNs in inhibiting the growth of MCMV in fibroblasts (11). In contrast, the replication of ΔM27-MCMV yielded 20-fold lower titers by IFN-α at 96 h p.i., confirming an enhanced antiviral effect. Most strikingly, a much more dramatic effect was observed with 500 U/ml IFN-γ, which inhibited ΔM27-MCMV replication almost completely by four orders of magnitude (Fig. 2 A). The reintroduction of *M27* into the ΔM27 genome (*M27*rev) restored the MCMV-WT phenotype against both IFNs. An increased sensitivity of ΔM27-MCMV versus *M27*rev was observed at concentrations as low as 3 U/ml IFN-γ (Fig. 2 B), confirming different dose responses for both viruses. In summary, the data proved that *M27* acts antagonistic to both IFN-α and IFN-γ.

pM27 down-regulates STAT2

To gain insight into the molecular mechanism of the pM27-dependent inhibition, we analyzed the overall levels of STAT molecules in cells infected with MCMV-WT, ΔM27-MCMV, and M27HA STAT2 was strongly down-regulated at 24 h p.i. (Fig. 3 A) and undetectable 48 h p.i in MCMV-WT– and M27rev-infected cells (unpublished data). In contrast, STAT2 was abundantly present in cells infected with the ΔM27-MCMV mutant. STAT2 mRNA was detected in equal amounts in Northern blots of MCMV-WT– and ΔM27-MCMV–infected cells (unpublished data), indicating intact STAT2 gene transcription in *M27*-expressing cells.

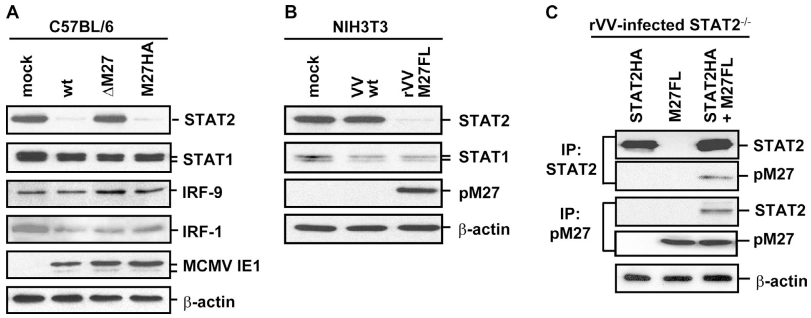

Figure 3. pM27 selectively affects STAT2. (A) pM27 down-regulates STAT2. C57BL/6-MEFs were either mock infected or infected with MCMV-WT, ΔM27-MCMV, or M27HA (10 PFU/cell each) for 24 h. Equivalent amounts of cell lysates were subjected to SDS-PAGE and analyzed by Western blot for STAT2, STAT1, IRF9/p48, IRF1, MCMV IE1/pp89, and β-actin. (B) NIH 3T3 were either mock infected, infected with VV-WT as a control, or infected with rVVM27FL (5 PFU/cell each). Cell lysates were prepared 16 h p.i. and analyzed by Western blot for STAT2, STAT1, pM27, and β-actin. (C) pM27 forms a complex with STAT2. *STAT2*$^{-/-}$ fibroblasts were infected with rVV expressing M27FL or STAT2-HA, or coinfected with both viruses (3 PFU/cell each). Cell lysates were prepared 8 h p.i. using an EMSA buffer, split into two aliquots, and subjected to immunoprecipitation using anti-HA and anti-FLAG antibodies, respectively. Immunoprecipitates were analyzed by Western blot for STAT2, pM27, and β-actin.

STAT1 was marginally down-regulated by all viruses 24 h p.i., whereas IFN response factor 9 (IRF9)/p48 was not affected (Fig. 3 A). Moreover, protein levels of IRF1, a factor critically involved in IFN-γ–induced MHC II expression and able to activate ISREs (15), were not affected by *M27* expression in MCMV-infected cells (Fig. 3 A). The STAT2-directed effect of pM27 was corroborated by the finding that the IFN-α–induced nuclear accumulation of STAT2 was intact in ΔM27-MCMV–infected cells but impaired by M27-HA-MCMV (unpublished data).

To investigate whether the selective expression of pM27 is sufficient to mediate the down-regulation of STAT2, we expressed the *M27*-FLAG sequence by a recombinant vaccinia virus (rVV), rVV-M27FL. STAT2 was found to be drastically reduced by rVV-M27FL but not by control VV-WT. No effect was observed with regard to STAT1 (Fig. 3 B). To test whether there is a physical interaction between pM27 and STAT2, the proteins were expressed by an rVV, either alone or together, and immunoprecipitated. A Western blot analysis of immunoprecipitates detected pM27 in anti-STAT2–precipitated material and vice versa after coexpression of both proteins (Fig. 3 C). STAT1 was not found in the pM27–STAT2 complex (unpublished data). The loss of STAT2 occurred also in *STAT1*$^{-/-}$ fibroblasts (reference 16; unpublished data) and thus affects STAT2 monomers, indicating that the molecular mechanism used by pM27 is thoroughly different from the parainfluenza virus V protein that recognizes only STAT1/STAT2 heterodimers (17). The results demonstrated that STAT2 is the principal and direct molecular target of pM27.

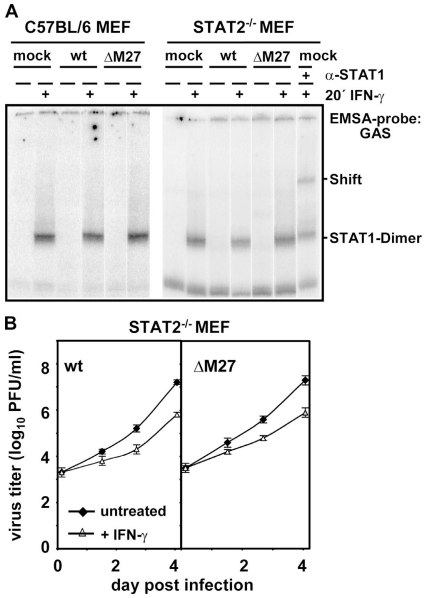

Figure 4. pM27 does not affect STAT1 but requires STAT2 for the inhibition of IFN-γ responses. (A) C57BL/6 MEFs and STAT2-deficient fibroblasts were infected with MCMV-WT or ΔM27-MCMV (10 PFU/cell each) for 24 h and exposed to 200 U/ml IFN-γ for 20 min. Equal protein amounts from 1:1 mixtures of nuclear and cytoplasmic cell extracts were evaluated by EMSA with a GAS probe (reference 21). Supershifting was performed by the addition of a STAT1-specific antibody before incubation with the probe. The mobility of STAT1 homodimers is indicated. (B) *STAT2*$^{-/-}$ fibroblasts were preincubated with 500 U/ml IFN-γ for 48 h, or not incubated before infection, with MCMV-WT and ΔM27-MCMV (0.01 PFU/cell each) for the indicated time. Titers of progeny virus were determined by a standard plaque assay.

The proviral effect of pM27 is strictly dependent on STAT2

According to current concepts, STAT1, but not STAT2, is required for IFNGR signaling (18, 19), although the levels of STAT1 expression are decreased in STAT2-deficient fibroblasts (20). To test whether pM27 has any effect on STAT1 that does not involve the degradation of STAT1, we analyzed the IFN-γ–induced DNA-binding activity of STAT1 by electrophoretic mobility shift assay (EMSA) in WT- and STAT2-deficient fibroblasts using a GAS-specific probe (21). As demonstrated in Fig. 4 A, STAT1 activation was intact in MCMV-WT and ΔM27-MCMV–infected MEFs, excluding the effects of pM27 on STAT1 phosphorylation, dimerization, and DNA binding. This held true in cells lacking STAT2, ruling out the possibility that STAT2 effected STAT1 function (Fig. 4 A). Moreover, the induction of IRF1 gene expression mediated by STAT1 dimers (γ-activated factor) was identical in MCMV-WT– and ΔM27-MCMV–infected cells (unpublished data). However, this result still leaves open the possibility that pM27 causes resistance to IFN-γ by acting on a target other than STAT2. To test whether pM27 is able to block IFNGR-dependent responses in the absence of STAT2, we studied MCMV-WT and ΔM27-MCMV replication in *STAT2*$^{-/-}$ fibroblasts (20). As shown in Fig. 4 B, the absence of STAT2 completely abolished the difference between MCMV-WT and ΔM27-MCMV, proving that STAT2 is a prerequisite to demonstrate any effect of pM27 on IFNGR signaling. This confirmed STAT2 as the only relevant target of pM27 for IFNGR signaling. Moreover, the reintroduction of STAT2 in *STAT2*$^{-/-}$ fibroblasts increased the sensitivity of ΔM27-MCMV but not MCMV-WT to IFN-α and, importantly, IFN-γ (unpublished data); however, the antiviral capacity of fibroblasts expressing endogenous STAT2 was clearly superior, confirming previous findings by Park et al. (20).

The antiviral efficiency of IFN-γ is contingent on type I IFN

IFNAR components and IFN-β production were suggested to enhance IFN-γ signaling under certain conditions through the association of the two non–ligand-binding receptor chains, IFNAR1 and IFNGR2 (22). To address the possibility that pM27 disrupts the cross talk between IFNRs by depleting STAT2, we determined the antiviral efficiency of IFN-γ in IFN-β–deficient primary MEF (Fig. 5 A). The antiviral efficiency of IFN-γ was strongly diminished (Fig. 5 A), but readily restored by the addition of exogenous IFN-α or IFN-β in a dose-dependent manner (Fig. 5 B). These data

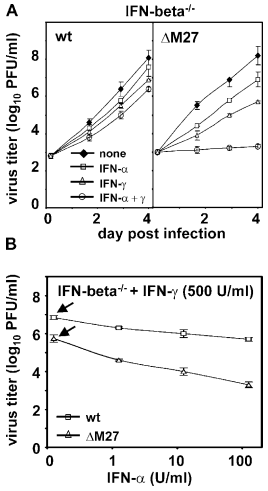

Figure 5. MCMV replication in IFN-β–deficient cells. (A) Primary IFN-β–deficient MEFs were infected with MCMV-WT and ΔM27-MCMV (0.01 PFU/cell each). Titers of the infectious virus were determined by a standard plaque assay. Growth curves were obtained after 48-h preincubation of cells without IFN, or with 500 U/ml IFN-α, 500 U/ml IFN-γ, or a combination of 100 U/ml IFN-α and 100 U/ml IFN-γ. (B) Primary IFN-β–deficient MEFs were treated with 500 U/ml IFN-γ in combination with graded concentrations of IFN-α and infected with MCMV-WT and ΔM27-MCMV (0.01 PFU/cell each). Viral titers obtained at 96 h p.i. were shown in relation to doses of IFN-α. The titers in the presence of IFN-γ and in the complete absence of type I IFN are highlighted by arrows.

indicate that a substantial part of the antiviral efficiency of IFN-γ depends on a synergistic action with type I IFNs (i.e., on IFN-β secretion and IFNAR1 signaling). However, the synergism of type I and type II IFNs could not explain the complete proviral effect of pM27. Importantly, in the absence of type I IFNs, the replication of ΔM27-MCMV was still more sensitive to IFN-γ compared with MCMV-WT, reaching 10-fold lower levels of progeny virus (Fig. 5 B). The fact that IFN-γ exerted an antiviral effect on ΔM27-MCMV replication in the absence of type I IFN function led us to conclude that STAT2 must also act as a direct mediator of IFN-γ responses.

STAT2 activation in response to IFN-γ

To assess the capacity of IFN-γ to activate STAT2 in the absence of IFNAR signaling, we analyzed protein phosphorylation on tyrosine after the treatment of IFNAR-deficient MEFs for various times with IFNs (Fig. 6 A). As expected, IFN-α and IFN-β failed to activate STAT2 in IFNAR1-deficient cells (Fig. 6 B and not depicted). In infected cells, STAT1 levels were slightly lower than in uninfected cells, and IFN-γ–dependent phosphorylation of STAT1 occurred in both ΔM27-MCMV– and in MCMV-WT–infected cells (Fig. 6 A). Notably, IFN-γ–induced tyrosine phosphorylation of STAT2 in IFNAR1-deficient cells was detectable within 5 min of incubation and increased to higher levels within 60 min of incubation (Fig. 6 A). The same result was obtained in ΔM27-MCMV–infected cells, whereas phosphorylated STAT2 was not detectable in MCMV-WT–infected cells (Fig. 6 A). The induction of STAT2 by IFN-γ did not occur in IFNGR1-deficient cells (Fig. 6 B), proving that STAT2 activation by IFN-γ is indeed coupled to IFNGR signaling. To test whether IFN-γ induces STAT2 phosphorylation in further cells, we analyzed a broad range

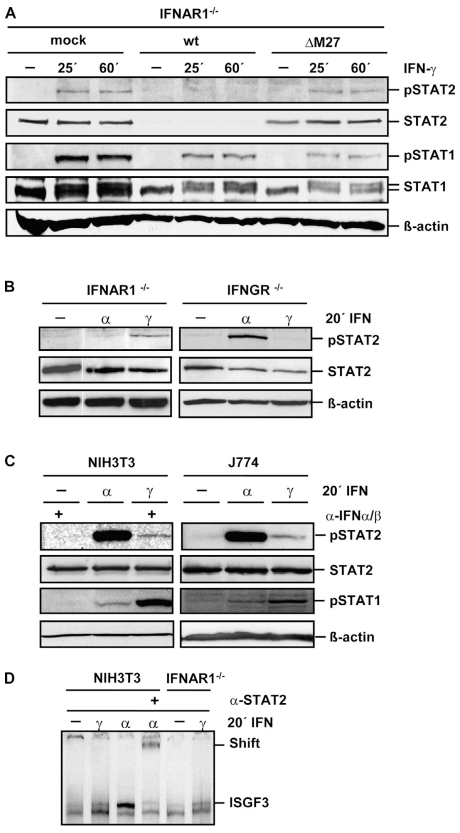

Figure 6. Phosphorylation of STAT2 in response to IFN-γ. (A) Primary IFNAR1-deficient MEFs were either mock infected or infected with MCMV-WT or ΔM27-MCMV (10 PFU/cell each) for 24 h before being exposed to 500 U/ml IFN-γ for the indicated time. Equivalent amounts of cell lysates were subjected to SDS-PAGE and analyzed by Western blot for p-Tyr^{689} STAT2, and reprobed for STAT2, p-Tyr^{701} STAT1, STAT1, and β-actin. (B) Primary IFNAR1- and IFNGR-deficient MEFs were either left untreated or treated with IFN-α (100 U/ml and 10 U/ml, respectively) or 500 U/ml IFN-γ for 20 min. Equivalent amounts of cell lysates were analyzed by Western blot for p-Tyr^{689} STAT2 and reprobed for STAT2 and β-actin. (C) NIH 3T3 fibroblasts and J774 macrophages were either left untreated or treated with 50 U/ml IFN-α or 500 U/ml IFN-γ for 20 min. 50 NU/ml type I neutralizing antibodies were added as indicated to remove endogenously produced IFN-β. Equivalent amounts of cell lysates were analyzed by Western blot for p-Tyr^{689} STAT2, and reprobed for STAT2, p-Tyr^{701} STAT1, and β-actin. (D) NIH 3T3 fibroblasts and IFNAR-deficient MEFs were not exposed or exposed to 500 U/ml IFN-γ or 50 U/ml IFN-α for 20 min. Equal protein amounts from 1:1 mixtures of nuclear and cytoplasmic cell extracts were evaluated by EMSA with an ISRE probe (reference 47). Supershifting was performed by the addition of a STAT2-specific antibody before incubation with the probe. The mobility of ISGF3 is indicated in the right margin.

of primary cells and cell lines. Although at clearly lower levels when compared with IFN-α, IFN-γ exposure of NIH 3T3 fibroblasts and J774 macrophages resulted in a rapid phosphorylation of STAT2 (Fig. 6 C), corroborating earlier experiments (23). The same type of result was also observed in BALB/c splenocytes, primary C57BL/6 MEFs, mouse SVEC endothelial cells, and human MRC5 fibroblasts (unpublished data). To determine whether the IFN-γ–mediated activation of STAT2 was sufficient to induce the formation of ISGF3 complexes and DNA binding, EMSA assays using an ISRE-specific probe were performed. As demonstrated in Fig. 6 D, the binding of ISGF3 to ISRE was observed in response to IFN-γ in NIH 3T3– and IFNAR1-deficient cells, confirming published data (24). The same result was seen in ΔM27-MCMV– but not MCMV-WT–infected cells (unpublished data), proving that IFN-γ induced STAT2 results in ISGF3-mediated signaling.

Considering the relatively low levels of STAT2 activation reached within 60 min of IFN-γ exposure versus the substantial inhibition achieved during two rounds of ΔM27-MCMV replication (Fig. 5), one could surmise that higher levels of phosphorylated STAT2 were generated during infection. To test this possibility, IFNAR-deficient cells were analyzed on extended IFN-γ treatment (Fig. 7 A). Unlike mock-infected cells, nucleoplasmic levels of phosphorylated STAT2 became strongly increased in ΔM27-MCMV–infected, IFNAR-deficient cells. Consequently, the formation and DNA binding of ISGF3 also accumulated over time in ΔM27-MCMV–infected, IFN-γ–exposed, IFNAR1-deficient cells (unpublished data). To assess the antiviral impact of STAT2 activation in the type I versus type II IFN–mediated inhibition of MCMV replication, we compared the yield of ΔM27-MCMV and MCMV-WT replication in MEFs deficient in STAT2, IFN-β, IFNGR, and IFNAR expressions in the presence of either 500 U/ml IFN-α or 500 U/ml IFN-γ at 96 h p.i. As demonstrated previously (Fig. 4 B), no difference in virus growth was observed for ΔM27-MCMV and MCMV-WT when replicating in IFN-α– and IFN-γ–treated, STAT2-deficient MEFs (Fig. 7 B). In agreement with the data presented in Fig. 5, ΔM27-MCMV replication was ∼13-fold lower in IFN-β–deficient cells treated with either exogenous IFN-α or IFN-γ when compared with MCMV-WT, demonstrating that STAT2 is implicated in both the type I and type II IFN pathways. IFN-α treatment of IFNAR-deficient cells did not influence ΔM27-MCMV growth when related to MCMV-WT replication, whereas IFN-γ blocked ΔM27-MCMV ∼20-fold better than MCMV-WT (Fig. 7 B). The enhanced inhibition of ΔM27-MCMV by IFN-γ was abolished in IFNGR-deficient cells, but evident when using IFN-α (Fig. 7 B). Considering that pM27 exclusively affects STAT2, these data demonstrate that both types of IFNs require STAT2 to block MCMV replication. In summary, the findings establish a STAT2- and ISGF3-dependent pathway of IFN-γ signaling for antiviral responses.

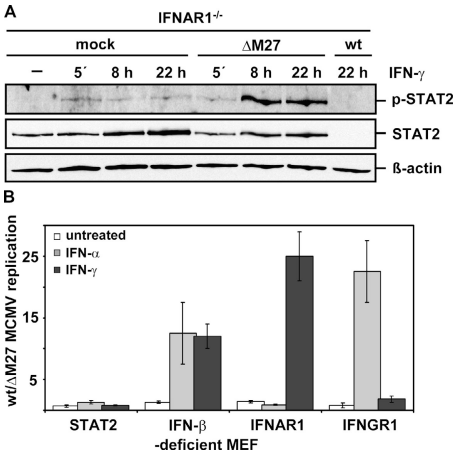

Figure 7. IFN-γ–induced increase of STAT2-P in ΔM27-infected cells and its impact for the inhibition of MCMV replication. (A) IFNAR1-deficient MEFs were either mock infected or infected with ΔM27-MCMV or MCMV-WT (10 PFU/cell each) for 24 h before exposed to 500 U/ml IFN-γ for the indicated time. Equivalent amounts of nucleoplasmic lysates were subjected to SDS-PAGE and analyzed by Western blot for p-Tyr^{689} STAT2, and reprobed for STAT2 and β-actin. (B) Comparative analysis of MCMV replication in MEF lacking components of the IFN signaling cascade. The indicated cells were incubated with 500 U/ml IFN-α or 500 U/ml IFN-γ for 48 h or left untreated before being infected with MCMV-WT or ΔM27-MCMV (0.01 PFU/cell each). The efficiency of MCMV replication is expressed as the ratio of virus yield at 96 h p.i., as determined by a standard plaque assay.

M27 is essential for MCMV replication in vivo, and replication of ΔM27-MCMV is restored in IFNAR- and IFNGR-deficient mice

To evaluate the significance of *M27* in vivo, ΔM27-MCMV and M27rev virus titers were determined in the major target organs of C57BL/6 (Fig. 8 A) and 129/Sv (unpublished data) mice. M27rev replicated in all tissues, reaching peak titers in the liver at 7–14 d and in the SGs at day 14, before MCMV growth was cleared in all organs except the SGs. In contrast, ΔM27-MCMV did not replicate in the liver and did not spread to the SGs. Thus, the deletion of *M27* resulted in a dramatic replication deficiency of MCMV in vivo, confirming published data (14). To dissect the relative impact of STAT2 activation by IFN−α/β and IFN-γ in vivo, we studied the absence of the *M27* expression in MCMV-infected IFNGR- and IFNAR-deficient mice. If the attenuated phenotype was because of a STAT2-dependent effect on IFNAR as well as IFNGR signaling, it is reasonable to assume that ΔM27-MCMV should replicate to higher titers in mice lacking IFNGR (25) and IFNAR, at least during the first days of infection before the onset of adaptive immunity. Replication of ΔM27-MCMV in IFNGR1-deficient mice reached titers in the liver comparable to those seen with M27rev at day 3 p.i. in C57BL/6 mice. Thereafter, ΔM27-MCMV was rapidly cleared in

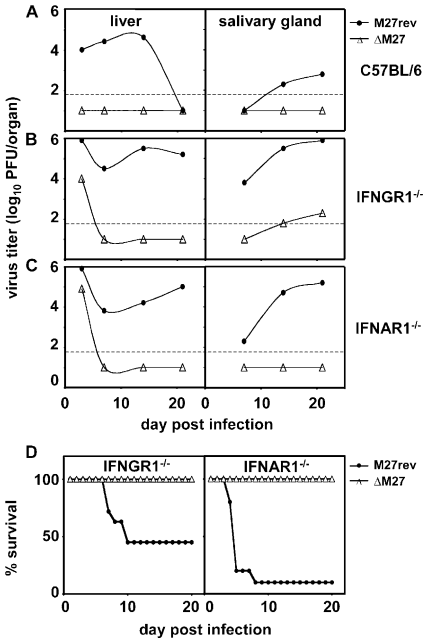

Figure 8. Analysis of ΔM27-MCMV and M27rev in vivo. (A) C57BL/6, (B) 129Sv(ev) *IFNGR1*$^{-/-}$ mice (reference 25), and (C) *IFNAR1*$^{-/-}$ mice backcrossed with C57BL/6 mice were infected i.p. with 2×10^5 PFU of tissue culture–derived ΔM27-MCMV or M27rev. Mice were killed at days 3, 7, 14, and 21, and organ titers of ΔM27-MCMV or M27rev in the liver and SGs were determined by a standard plaque assay. Each value represents the median of total SG titers or 1 g of liver from five infected animals. The dotted line shows the detection limit of organ titration (<100 PFU/gram of organ). (D) *IFNAR1*$^{-/-}$ and *IFNGR1*$^{-/-}$ mice ($n = 10$ per group) were infected i.v. with 5×10^6 PFU of the indicated virus and monitored for survival over time.

IFNGR1-deficient mice but able to spread to the SGs (Fig. 8 B). The data suggest that control of ΔM27-MCMV in IFNGR-KO mice is mediated through a STAT2-dependent pathway of type I IFN that is intact in IFNGR-deficient mice but blocked by M27rev. Likewise, ΔM27-MCMV, but not MCMVrev, was rapidly cleared in IFNAR1-deficient mice after an initial phase of replication at day 3 p.i and failed to establish an infection in the SGs (Fig. 8 C), which is compatible with an IFN-γ–mediated control of viral replication depending on STAT2. In summary, replication in the initial stages of infection in mice correlated with the relative productivity of ΔM27-MCMV and M27rev observed in IFN-treated, IFNR-deficient fibroblasts (Fig. 7 B), although the relative usage of individual IFN pathways cannot be assessed in vivo. At later stages, ΔM27-MCMV replication was controlled in both IFNAR1 and IFNGR1-deficient animals, whereas M27rev replicated to very high titers in all organs (Fig. 8, B and C).

In a further set of experiments, higher virus doses were administered intravenously. Under these conditions, M27rev caused a lethal infection in 90% of IFNAR1-deficient mice and ~50% of IFNGR1-deficient mice (Fig. 8 D), respectively, confirming previously published data (7). Deletion of *M27* resulted in the complete survival of both IFNAR1- and IFNGR1-KO mice, indicating that STAT2-dependent functions induced by IFN-γ or type I IFNs can protect against lethal infection in vivo.

DISCUSSION

Based on a systematic approach of forward mutagenesis using the random transposon insertion into a CMV–BACmid and the screening of mutants with an IFN-sensitive reporter gene, this study identifies the long sought after CMV antagonist of IFNR signaling. The Tn insertion found in three independent mutants guided the search to a single gene, *M27*, as a causal principle. This gene is conserved between all *β-herpesvirinae*. Remarkably, we discovered that the *M27*-encoded, 79-kD protein blocked both IFN-α/β and IFN-γ responses via STAT2 and, thus, has a huge impact on viral fitness in vivo. The selective removal of the STAT2 protein by pM27 is executed via the ubiquitin–proteasome pathway of protein degradation (unpublished data). In this study, we took advantage of a panel of targeted, single gene KO host cells and used pM27 as a selective tool to allow the dissection of STAT2-dependent antiviral effects. This combined approach provided the unique opportunity to assess the relative impact of IFNs and their intracellular signal transduction pathways with regard to their antiviral potency.

pM27 substrate specificity

According to the current understanding, STAT1, but not STAT2, has a central role in both IFNAR and IFNGR signaling (2, 4, 18, 19, 26). The inhibition of STAT1, which represents a common component between the IFN-α/β and the IFN-γ signaling pathways, is an obvious strategy for a virus that causes infected cells to resist the action of IFNs regardless of whether the IFNs were produced by infected cells or activated immune cells. Indeed, several viruses, including members of *Paramyxoviridae*, follow this principle (26). Therefore, the specificity of pM27 for its cellular target, STAT2, deserves comment. Considering the relative resistance of MCMV replication against IFN-γ and IFN-α conferred by pM27, our findings come as a surprise. Most indicators reveal that pM27 has an exquisite specificity for monomeric STAT2, but not for STAT1, supported by evidence such as: (a) both mouse and human STAT2, but not STAT1, were down-regulated; no effect was seen with regard to STAT3 and STAT4 (unpublished data), which have also been implicated in IFNR signaling (for review see reference 19); (b) pM27 forms a physical complex with STAT2 but not STAT1; (c) the nuclear accumulation of STAT2, but not STAT1, was affected (unpublished data); (d) the IFN-γ–induced DNA-binding activity of STAT1 was intact in MCMV-infected fibroblasts; and (e) most important, ΔM27-MCMV replicates as efficiently as MCMV-WT in response to IFN-γ in STAT2-deficient fibroblasts (Fig. 5 B), indicating that the proviral activity of pM27 depends exclu-

sively on STAT2 expression. A moderate decrease of STAT1 protein levels in MCMV-infected cells occurred independently of *M27*, pointing to an additional viral function undermining IFN responsiveness.

STAT2 activation by IFN-γ

STAT2 has a well-established role as an essential mediator of signal transduction through the type I IFNR because of its incorporation into ISGF3 complexes (19, 20, 26). Our findings provide several lines of evidence indicating that STAT2 plays an additional role after triggering the IFNGR. First, STAT2 is activated by IFN-γ in a broad range of cell types, as indicated by tyrosine phosphorylation. Second, STAT2 activation is abolished in IFNGR-deficient cells. Third, IFN-γ induces ISGF3 complex formation and DNA binding. Fourth, IFN-γ exerted a pM27-dependent antiviral activity when acting in the complete absence of type I IFNs (i.e., in IFNAR1-deficient and IFN-β–deficient cells). Fifth, cellular genes known to be activated by IFN-γ (e.g., the immunoproteasome subunits LMP2, LMP7, and MECL1) are inducible in ΔM27-MCMV–infected, but blocked in MCMV-WT–infected, cells (27). And sixth, MCMV replication and the outcome of infection in IFNAR1-deficient mice (with intact IFNGR expression) were dependent on pM27, suggesting that STAT2 plays a decisive antiviral role for IFNGR-mediated responses in vivo. Notably, our findings are not completely unprecedented. A previous study reported an impaired inhibition of vesicular stomatitis virus replication by IFN-γ in STAT2-deficient cells (20). This result was interpreted to be caused by an impaired autocrine loop in which IFN-γ promotes its antiviral activity by the induction of type I IFNs (20). Based on our finding that STAT2 activation in response to IFN-γ occurs within minutes, we can exclude this explanation. The fact that IFN-γ induces STAT2 phosphorylation in many types of cells (Fig. 7 B), raises the possibility that this signaling pathway is of broad significance for various tissues and is critical for the control of a variety of viral pathogens. Clearly, further components of this IFNGR-coupled signaling pathway remain to be elucidated (e.g., the IFNGR-associated tyrosine kinase[s], which recognize STAT2 as a substrate). One candidate kinase is represented by JAK1, which is associated with IFNGR and was demonstrated to be able to mediate tyrosine phosphorylation of STAT2 when expressed in insect cells (28).

It is self-evident that the different degrees of STAT2 activation by type I versus type II IFN cannot simply be translated into its relative antiviral effectiveness. IFN-γ generates relatively low levels of activated STAT2 in normal cells, which explains why this pathway escaped attention in the past. Guided by a clear pM27- and STAT2-dependent phenotype of MCMV replication, we discovered high levels of phosphorylated STAT2 in ΔM27-MCMV–infected cells within hours of IFN-γ exposure without any involvement of IFNAR signaling (Fig. 7 A). At first glance, the activation of STAT2 by IFN-γ, resulting in ISGF3 formation, might appear simply redundant with the stronger induction of this transcription complex by type I IFNs. Instead, the intrinsic capacity of IFNGR to induce not only STAT1 dimers, but also STAT2 phosphorylation and thus ISGF3 autonomously, is of great biological advantage. A large number of viruses, including HCMV (29) and many RNA viruses, are able to repress the transcriptional activation of type I IFN genes, and poxviruses prevent the binding of secreted type I IFNs to IFNAR (26). Such countermeasures foil the attempt to induce ISGF3; i.e., the autocrine loop of type I IFNs enhancing IFN-γ. In such a scenario, ISGF3 activation by IFN-γ, even at lower levels, may provide a substantial qualitative, as well as a quantitative, augmentation of IFNGR/GAS-driven transcriptional responses and represent a decisive adaptive strategy of the antiviral defense. As demonstrated in MCMV-infected, IFNAR-deficient mice, this antiviral mechanism can protect from lethal disease (Fig. 8 D). On the other hand, IGSF3 becomes an attractive target for viral interference because it is of utmost importance for IFNAR as well as IFNGR signaling. Remarkably, HCMV shares this strategy with MCMV by down-regulating the third component of ISGF3, IRF9/p48 (30).

The proviral effect of pM27 on MCMV replication was particularly prominent in cells pretreated with high doses of IFNs; i.e., after the complete activation of the IFN-mediated pathways and the establishment an antiviral state. From this observation, we must conclude that the maintenance of the antiviral state critically requires an intact and permanent function of STAT2. This implies that the antiviral state, by itself, is not a long-lasting biological condition but is readily reversed when IFNR signaling is disrupted.

pM27 disruption of type I and type II IFN synergy

Another prominent finding of our study is the fact that IFN-γ relies in part on type I IFNs to achieve a potent antiviral response. This effect requires only minute amounts of type I IFNs (Fig. 5) and may explain the antiviral synergism that has been observed with other herpesviruses like HSV (31). The required levels of IFN-α/β are easily achieved either by virus induction and/or by IFN-γ itself, which induces type I IFNs (32). In fact, the antiviral activity of IFN-γ in cells with the capacity to establish the autocrine type I IFN loop may generally include the synergistic effect of type I IFNs. Only the complete withdrawal of any IFN-α/β secretion or the prevention of signaling (e.g., in IFNAR-deficient cells) discloses the relatively weak antiviral response exerted by IFN-γ alone. Therefore, although the disruption of STAT2 by pM27 only demonstrates a moderate effect with regard to the antiviral potency of type I IFNs, it has much more dramatic consequences for the antiviral efficiency of IFN-γ. The augmentation of type II by type I IFNs is unidirectional, as the IFN-α–mediated inhibition in IFNGR1-deficient cells is not affected (22, 27).

According to classical concepts, IFNAR and IFNGR have been considered as separate receptor complexes, with

each activating a specific set of STAT proteins (2, 4, 18, 19). Several explanations for the IFN synergy observed here are possible. The cross communication of both IFNs could operate as molecular cross talk between non–ligand-binding IFNR components (i.e., IFNAR1 and IFNGR2), which were proposed to directly interact in caveolar membranes and thus couple both receptor pathways (22). There is evidence that STAT2 as well as STAT1 are indeed physically associated with IFNAR1 and IFNGR2 after IFN-γ treatment (22), providing a possible pM27 checkpoint to interfere with. In addition, the synergy between both pathways may be achieved at a transcriptional level by potentiating the transcriptional activation of antiviral genes because of a concerted action of γ-activated factor and ISGF3.

By using pM27 to attack a single molecular target, STAT 2, MCMV performs the dual function of withstanding type I and type II IFNs. By depleting STAT2, pM27 gains control over IFNR signaling by (a) disrupting IFNAR signal transduction; (b) preventing the synergy of type I IFNs with IFN-γ, which is of primary importance for MCMV replication; and (c) blocking the downstream signals induced by a direct activation of STAT2 by IFN-γ. In addition, pM27 may even affect GAS-dependent responses by reducing the expression level of STAT1, which is controlled by STAT2 (20).

Consequences of *M27* expression for MCMV immunity

Besides its direct activity in promoting virus replication in the presence of IFNs, pM27 is also likely to have immunomodulatory proviral effects. IFN-γ stimulates a multitude of genes implicated in antigen presentation, cell adhesion, chemotaxis, and inflammation (33). In fact, the antiviral effector function of both $CD8^+$ and $CD4^+$ T cells depends critically on IFN-γ (5, 8, 34). Replicating under the permanent and selective pressure of IFNs, CMVs have developed gene functions that counteract IFN-induced gene expression. CMV-infected cells were shown to resist IFN-γ–induced MHC class II expression, transcriptional activation, and antigen presentation to $CD8^+$ T cells (8, 10, 12, 35-37). Therefore, it is conceivable that Δ*M27*-MCMV–infected cells differ from *M27*-expressing cells with regard to antigen presentation. In fact, the expression of IFN-γ–inducible proteasome subunits, which is prevented in MCMV-WT infected cells, is at least partially restored in the absence of *M27* (27). Such differences may explain our observation that the initial restoration of ΔM27-MCMV replication in IFNR-deficient mice is rapidly cleared at later time points of infection when T cell responses are mounted. Conversely, *M27*-expressing MCMV achieves a sustained phase of replication, demonstrating that STAT2 constitutes an important target whose selection is required to gain a window of opportunity for viral replication and spread in an IFN-producing environment.

MATERIALS AND METHODS

MCMV infection of mice and plaque assay for the detection of MCMV in tissues. C57BL/6 and *IFNAR1*$^{-/-}$ (provided by S.H.E. Kaufmann, Max-Planck-Institute for Infection Biology, Berlin, Germany) backcrossed with C57BL/6 mice and *IFNGR1*$^{-/-}$ mice (25) were bred in the Central Animal Facility of Rijeka University, in accordance with the guidelines contained in the International Guiding Principles for Biomedical Research Involving Animals. The Ethical Committee at the University of Rijeka approved all animal experiments. 6–8-wk-old mice were infected i.p. with 2×10^5 PFU of tissue culture–derived ΔM27-MCMV or M27rev diluted in a volume of 500 μl. Mice were killed at day 3, 7, 14, or 21 p.i., and the organs were frozen immediately at −70°C. The titer of infectious virus was determined by titrating organ homogenates of liver and SGs using a standard plaque assay (6).

Cells. Primary MEFs of C57BL/6, *IFNAR1*$^{-/-}$, *IFNGR1*$^{-/-}$, or *IFN-β*$^{-/-}$ mice (provided by T. Leanderson, Lund University, Lund, Sweden; reference 38) were prepared as previously described (39). MEFs were maintained in DMEM supplemented with 10% FCS, penicillin, and streptomycin, and 2 mM glutamine, and they were used for subsequent experiments within three passages. Murine *STAT1*$^{-/-}$ cells (provided by D. Levy, New York University School of Medicine, New York, NY; reference 16), SVEC (CRL-2181), J774 macrophages (TIB-67), human MRC-5 fibroblasts (CCL-171; all three from American Type Culture Collection), and CV1 cells were grown in DMEM with 10% FCS. For the culture of NIH 3T3 (CRL1658; American Type Culture Collection), 3T3-ISRE-luc cells (provided by E. Hellebrand, Max von Pettenkofer-Institut, Munich, Germany) and *STAT2*$^{-/-}$ fibroblasts (provided by C. Schindler, Columbia University, New York, NY; reference 20), FCS was replaced with 5% normal calf serum.

Viruses, IFN conditions, and virus replication analysis. The MCMV-WT viruses used were either MCMV strain Smith or the BAC-derived WT recombinant MW97.01 with WT properties in vitro and in vivo (40). Viable MCMV random Tn insertion mutants were retrieved from a library of Tn*Max*16 containing MCMV BACs after the transfection of NIH 3T3 cells (13). The Tn insertion site was determined by DNA sequencing as described previously (41). Virus stocks were prepared and virus titers were measured by a standard plaque assay on MEFs. MCMV infection was enhanced by centrifugation at 800 *g* for 30 min. The selective expression of MCMV immediate early gene products was achieved as described previously (8). Late phase gene expression was prevented by 250 μg/ml phosphonoacetic acid. For the replication analysis, MEFs in passage 2 were infected with 0.01 PFU/cell MCMV and frozen at −70°C at the time points indicated in Figs. 2 A, 4 B, and 5 A. Susceptibility to IFNs was assayed by virus growth in the presence of recombinant mouse IFN-α or IFN-γ (PBL Biomedical Laboratories) after preincubation with IFNs for 48 h before infection. In some experiments, type I IFN neutralizing antibodies (PBL Biomedical Laboratories) were used. The infection of subconfluent 3T3 or *STAT1*$^{-/-}$ cells with VV was performed overnight with 5 PFU/cell. VV titers were measured by plaque assay on CV1 cells.

BAC-based mutagenesis and construction of recombinant MCMV viruses. Recombinant MCMV were generated according to a previously published procedure (42) using the BAC plasmid pSM3fr (40). For the construction of the ΔM27-MCMV mutant, a PCR fragment was generated from the contiguous primers 5′-M27 (5′-ATATTCCTCCTGTCTTCCGTGTGTCGCTCGTGTCCTGTCACGTCGTGGAATGCCTTCGATTC-3′) and 3′-DEL-M27 (5′-GGAAAAAGACGACGGTGTCATTTATCGACGGCGCCGTGTCGCGCTGACCACAAGGACGACGACGACAAGTAA-3′) using the plasmid pSLFRTKn (43) as template DNA. For the 3′-terminal addition of the HA-tag sequence to the *M27* ORF, a PCR fragment was generated using the same template and the primers 5′-M27 and 3′-M27-HA(5′-GATGATGGCGGCGAGTCCGACGGCTCCGAGTTTGTGGTGGAGCGGGTGTACCCATACGATGTTCCAGATTACGCGTGAACAAGGACGACGACGACAAGTAA-3′ (HA sequence underlined). The PCR fragments containing a kanamycin resistance gene were inserted into pSM3fr by homologous recombination in *Escherichia coli,* leading to replacement of the *M27* gene stop codon by the HA sequence.

The Kn^r was excised from both BACs by FLP-mediated recombination (42), generating the MCMV BACs pSM3fr-M27HA and pSM3fr-ΔM27. The M27rev virus was constructed from a 5.2-kb KpnI fragment (nt 30293–35480) containing the *M27* gene and flanking homologies subcloned into the shuttle vector pST76KSR (provided by M. Messerle, Hannover Medical School, Hannover, Germany). The *M27* gene from plasmid pST76KSR-M27 was inserted into pSM3fr-ΔM27 by two-step homologous recombination (44), resulting in the BAC pSM3fr-M27rev. The correct mutagenesis of all recombinant MCMV BACs was confirmed by a restriction analysis and the sequencing of the M27 genome region. The recombinant viruses ΔM27-MCMV, M27HA, and M27rev were reconstituted by the transfection of MEF using Superfect reagent (QIAGEN). Residual BAC sequences were removed by sequential cell culture passages as previously described (40).

Generation of VV recombinants (rVV). The *M27* ORF was amplified from MCMV using the primers az-M27-1 (5′-CTCTCT*AGATCT*-GACCATGGCGGACCG-3′) and az-M27-F2 (5′-CACA*GAATTC*TGC-AGTCACTTGTCGTCGTCCTTGTAGTCCACCCGCTCCACC-ACAAACTC-3′). Primer az-M27-1 contains a BglII site (in italics), and az-M27-F2 contains an EcoRI site (in italics) and the coding sequence for the FLAG epitope (underlined). The PCR fragment was cloned into the vaccinia expression vector p7.5k, resulting in p7.5K131-M27FL, which was used to generate rVVM27FL after homologous recombination into the thymidine kinase locus of vaccinia strain Copenhagen as described previously (45). For the generation of rVVSTAT2HA, the STAT2 gene was subcloned from pRC-STAT2 (a gift from C. Schindler) into p7.5K131. The HA tag was added using the primers az-STAT2-1 (5′-TTCCTCTATCCCCGAATCCCTC-3′) and az-STAT2-HA2 (5′-CGGGGTACCTCACGCGTAATCTGGAACA-TCGTATGGGTACGCAGCGTCCTTAGAAGGTATCAAGAG-3′) containing the HA coding sequence (underlined). The rVVs were isolated by selection with BrDU using tk^- 143 cells.

Reporter gene assays. 3T3-ISRE-luc cells were selected after cotransfection with pcDNA1-neo (Invitrogen) and pISRE (Stratagene) containing five copies of an ISRE consensus sequence upstream of the firefly luciferase gene, and then cultured in the presence of 100 μg/ml G418. For reporter gene assays, either uninfected cells or MCMV-infected cells (10 PFU/cell) were induced with recombinant mouse IFN-α for 5 h and harvested in lysis buffer. Luciferase activity was then measured according to the manufacturer's instructions (Roche) using a microplate luminometer (model LB 96 V; Berthold).

EMSA, immunoblot analysis, and immunoprecipitation. Extractions were performed according to established protocols (46). Cells were infected (10 PFU/cell) and washed before being lysed in cytosolic extraction buffer (10 mM KCl, 20 mM Hepes, 0.2% NP-40, 0.1 mM EDTA, 10% glycerol, 0.1 mM vanadate, 0.1 mM PMSF, 1 mM dithiothreitol, and complete protease inhibitors, pH 7.4; Roche). The extracts were spun at 16,000 *g* for 16 s at 4°C. The supernatants were collected, spun for 10 min, and used as cytosolic extracts for EMSA and immunoblot. The pellets were washed in PBS and suspended in nuclear extraction buffer (420 mM KCl, 20 mM Hepes, 0.1 mM vanadate, 20% glycerol, 1 mM EDTA, 0.1 mM PMSF, 1 mM dithiothreitol, and complete protease inhibitors, pH 7.6). After incubation on ice for 30 min, the extracts were spun at 16,000 *g* for 20 min at 4°C, and the supernatants were used as nuclear extracts. A 1:1 mix of nuclear and cytosolic lysate was incubated with 1 ng of ^{32}P-labeled M67 GAS (21) or ISG15 ISRE probe (47) for 5 min at room temperature. The binding activity was visualized by a phosphoimaging system (model Storm 820; Molecular Dynamics). The supershift was performed with rabbit antiserum recognizing STAT1 (E23; Santa Cruz Biotechnology, Inc.) or murine STAT2 (20).

For immunoblotting, equal amounts of cell lysate were suspended in a Laemmli sample buffer. Proteins were separated by SDS-PAGE and transferred to nitrocellulose filters. Immunoblot analyses were performed with anti-HA–specific rat mAb 3F10 (Roche), anti-FLAG–specific mouse mAb M2 (Sigma-Aldrich), monoclonal mouse anti–β-actin (Sigma-Aldrich), mouse mAb raised against MCMV pp89 (CROMA 101), rabbit antiserum specific for STAT1 (E23) or murine STAT2 (provided by C. Schindler; reference 20), antiserum against IRF9/p48 (C20; Santa Cruz Biotechnology, Inc.), IRF1 (M20; Santa Cruz Biotechnology, Inc.), and mAb recognizing p-Tyr^{701} STAT1 (A2; Santa Cruz Biotechnology, Inc.) or p-Tyr^{689} STAT2 (Tyr 689; Upstate Biotechnology). Proteins were visualized using the ECL-Plus chemiluminescence system (GE Healthcare). Immunoprecipitation was performed as previously described (48) using anti-HA or anti-FLAG antibodies after cell lysis using EMSA buffer.

We are grateful to T. Ziade for help with experiments in the initial phase of the study. We thank K. Wichmann and B. Bauer for technical assistance, H. Reinhard for constructing rVVM27FL, E. Hellebrand for 3T3-ISRE-luc, and A. Halenius and T. Meyer for expert experimental advice. We are grateful to C. Schindler, D. Levy, T. Leandersson, M. Messerle, and S.H.E. Kaufmann for providing reagents and to U. Vinkemeier for reading the manuscript.

This work was supported by grants from the Deutsche Forschungsgemeinschaft (SFB 421A8 and SFB 455A7) and the European Union (QLRT-2001-01112).

The authors have no conflicting financial interests.

Submitted: 12 July 2004
Accepted: 25 March 2005

REFERENCES

1. Darnell, J.E., Jr. 1997. STATs and gene regulation. *Science*. 277:1630–1635.
2. Stark, G.R., I.M. Kerr, B.R. Williams, R.H. Silverman, and R.D. Schreiber. 1998. How cells respond to interferons. *Annu. Rev. Biochem.* 67:227–264.
3. Li, X., S. Leung, I.M. Kerr, and G.R. Stark. 1997. Functional subdomains of STAT2 required for preassociation with the alpha interferon receptor and for signaling. *Mol. Cell. Biol.* 17:2048–2056.
4. Bach, E.A., M. Aguet, and R.D. Schreiber. 1997. The IFN gamma receptor: a paradigm for cytokine receptor signaling. *Annu. Rev. Immunol.* 15:563–591.
5. Lucin, P., I. Pavic, B. Polic, S. Jonjic, and U.H. Koszinowski. 1992. Gamma interferon–dependent clearance of cytomegalovirus infection in salivary glands. *J. Virol.* 66:1977–1984.
6. Polic, B., H. Hengel, A. Krmpotic, J. Trgovcich, I. Pavic, P. Luccaronin, S. Jonjic, and U.H. Koszinowski. 1998. Hierarchical and redundant lymphocyte subset control precludes cytomegalovirus replication during latent infection. *J. Exp. Med.* 188:1047–1054.
7. Presti, R.M., J.L. Pollock, A.J. Dal Canto, A.K. O'Guin, and H.W. Virgin IV. 1998. Interferon gamma regulates acute and latent murine cytomegalovirus infection and chronic disease of the great vessels. *J. Exp. Med.* 188:577-588.
8. Hengel, H., P. Lucin, S. Jonjic, T. Ruppert, and U.H. Koszinowski. 1994. Restoration of cytomegalovirus antigen presentation by gamma interferon combats viral escape. *J. Virol.* 68:289–297.
9. Hengel, H., W. Brune, and U.H. Koszinowski. 1998. Immune evasion by cytomegalovirus–survival strategies of a highly adapted opportunist. *Trends Microbiol.* 6:190–197.
10. Heise, M.T., M. Connick, and H.W. Virgin IV. 1998. Murine cytomegalovirus inhibits interferon γ–induced antigen presentation to CD4 T cells by macrophages via regulation of expression of major histocompatibility complex class II–associated genes. *J. Exp. Med.* 187: 1037–1046.
11. Lucin, P., S. Jonjic, M. Messerle, B. Polic, H. Hengel, and U.H. Koszinowski. 1994. Late phase inhibition of murine cytomegalovirus replication by synergistic action of interferon-gamma and tumour necrosis factor. *J. Gen. Virol.* 75:101–110.
12. Miller, D.M., B.M. Rahill, J.M. Boss, M.D. Lairmore, J.E. Durbin, J.W. Waldman, and D.D. Sedmak. 1998. Human cytomegalovirus inhibits major histocompatibility complex class II expression by disruption of the JAK–STAT pathway. *J. Exp. Med.* 187:675–683.
13. Brune, W., C. Menard, J. Heesemann, and U.H. Koszinowski. 2001.

A ribonucleotide reductase homolog of cytomegalovirus and endothelial cell tropism. *Science*. 291:303–305.
14. Abenes, G., M. Lee, E. Haghjoo, T. Tong, X. Zhan, and F. Liu. 2001. Murine cytomegalovirus open reading frame M27 plays an important role in growth and virulence in mice. *J. Virol.* 75:1697–1707.
15. Taniguchi, T., K. Ogasawara, A. Takaoka, and N. Tanaka. 2001. IRF family of transcription factors as regulators of host defense. *Annu. Rev. Immunol.* 19:623–655.
16. Marie, I., J.E. Durbin, and D.E. Levy. 1998. Differential viral induction of distinct interferon-alpha genes by positive feedback through interferon regulatory factor-7. *EMBO J.* 17:6660–6669.
17. Parisien, J.P., J.F. Lau, J.J. Rodriguez, B.M. Sullivan, A. Moscona, G.D. Parks, R.A. Lamb, and C.M. Horvath. 2001. The V protein of human parainfluenza virus 2 antagonizes type I interferon responses by destabilizing signal transducer and activator of transcription 2. *Virology*. 283:230–239.
18. Aaronson, D.S., and C.M. Horvath. 2002. A road map for those who know JAK-STAT. *Science*. 296:1653–1655.
19. Kisseleva, T., S. Bhattacharya, J. Braunstein, and C.W. Schindler. 2002. Signaling through the JAK/STAT pathway, recent advances and future challenges. *Gene*. 285:1–24.
20. Park, C., S. Li, E. Cha, and C. Schindler. 2000. Immune response in Stat2 knockout mice. *Immunity*. 13:795–804.
21. Haspel, R.L., M. Salditt-Georgieff, and J.E. Darnell Jr. 1996. The rapid inactivation of nuclear tyrosine phosphorylated Stat1 depends upon a protein tyrosine phosphatase. *EMBO J.* 15:6262–6268.
22. Takaoka, A., Y. Mitani, H. Suemori, M. Sato, T. Yokochi, S. Noguchi, N. Tanaka, and T. Taniguchi. 2000. Cross talk between interferon-gamma and -alpha/beta signaling components in caveolar membrane domains. *Science*. 288:2357–2360.
23. Karaghiosoff, M., H. Neubauer, C. Lassnig, P. Kovarik, H. Schindler, H. Pircher, B. McCoy, C. Bogdan, T. Decker, G. Brem, et al. 2000. Partial impairment of cytokine responses in Tyk2-deficient mice. *Immunity*. 13:549–560.
24. Matsumoto, M., N. Tanaka, H. Harada, T. Kimura, T. Yokochi, M. Kitagawa, C. Schindler, and T. Taniguchi. 1999. Activation of the transcription factor ISGF3 by interferon-gamma. *Biol. Chem.* 380:699–703.
25. Muller, U., U. Steinhoff, L.F. Reis, S. Hemmi, J. Pavlovic, R.M. Zinkernagel, and M. Aguet. 1994. Functional role of type I and type II interferons in antiviral defense. *Science*. 264:1918–1921.
26. Goodbourn, S., L. Didcock, and R.E. Randall. 2000. Interferons: cell signalling, immune modulation, antiviral response and virus countermeasures. *J. Gen. Virol.* 81:2341–2364.
27. Khan, S., A. Zimmermann, M. Basler, M. Groettrup, and H. Hengel. 2004. A cytomegalovirus inhibitor of gamma interferon signaling controls immunoproteasome induction. *J. Virol.* 78:1831–1842.
28. Gupta, S., H. Yan, L.H. Wong, S. Ralph, J. Krolewski, and C. Schindler. 1996. The SH2 domains of Stat1 and Stat2 mediate multiple interactions in the transduction of IFN-alpha signals. *EMBO J.* 15:1075–1084.
29. Child, S.J., S. Jarrahian, V.M. Harper, and A.P. Geballe. 2002. Complementation of vaccinia virus lacking the double-stranded RNA-binding protein gene E3L by human cytomegalovirus. *J. Virol.* 76: 4912–4918.
30. Miller, D.M., Y. Zhang, B.M. Rahill, W.J. Waldman, and D.D. Sedmak. 1999. Human cytomegalovirus inhibits IFN-alpha–stimulated antiviral and immunoregulatory responses by blocking multiple levels of IFN-alpha signal transduction. *J. Immunol.* 162:6107–6113.
31. Sainz, B., Jr., and W.P. Halford. 2002. Alpha/Beta interferon and gamma interferon synergize to inhibit the replication of herpes simplex virus type 1. *J. Virol.* 76:11541–11550.
32. Zhou, A., Z. Chen, J.A. Rummage, H. Jiang, M. Kolosov, I. Kolosova, C.A. Stewart, and R.W. Leu. 1995. Exogenous interferon-gamma induces endogenous synthesis of interferon-alpha and -beta by murine macrophages for induction of nitric oxide synthase. *J. Interferon Cytokine Res.* 15:897–904.
33. Boehm, U., T. Klamp, M. Groot, and J.C. Howard. 1997. Cellular responses to interferon-gamma. *Annu. Rev. Immunol.* 15:749–795.
34. Geginat, G., T. Ruppert, H. Hengel, R. Holtappels, and U.H. Koszinowski. 1997. IFN-gamma is a prerequisite for optimal antigen processing of viral peptides in vivo. *J. Immunol.* 158:3303–3310.
35. Cebulla, C.M., D.M. Miller, Y. Zhang, B.M. Rahill, P. Zimmerman, J.M. Robinson, and D.D. Sedmak. 2002. Human cytomegalovirus disrupts constitutive MHC class II expression. *J. Immunol.* 169:167–176.
36. Miller, D.M., Y. Zhang, B.M. Rahill, K. Kazor, S. Rofagha, J.J. Eckel, and D.D. Sedmak. 2000. Human cytomegalovirus blocks interferon-gamma stimulated up-regulation of major histocompatibility complex class I expression and the class I antigen processing machinery. *Transplantation*. 69:687–690.
37. Popkin, D.L., M.A. Watson, E. Karaskov, G.P. Dunn, R. Bremner, and H.W. Virgin. 2003. Murine cytomegalovirus paralyzes macrophages by blocking IFN-γ–induced promoter assembly. *Proc. Natl. Acad. Sci. USA*. 100:14309–14314.
38. Erlandsson, L., R. Blumenthal, M.L. Eloranta, H. Engel, G. Alm, S. Weiss, and T. Leanderson. 1998. Interferon-beta is required for interferon-alpha production in mouse fibroblasts. *Curr. Biol.* 8:223–226.
39. Brune, W., H. Hengel, and U.H. Koszinowski. 1999. A mouse model for cytomegalovirus infection. *In* Current Protocols in Immunology. J.E. Coligan, editor. John Wiley & Sons, Inc. New York, 19.7.1–19.7.13.
40. Wagner, M., S. Jonjic, U.H. Koszinowski, and M. Messerle. 1999. Systematic excision of vector sequences from the BAC-cloned herpesvirus genome during virus reconstitution. *J. Virol.* 73:7056–7060.
41. Hobom, U., W. Brune, M. Messerle, G. Hahn, and U.H. Koszinowski. 2000. Fast screening procedures for random transposon libraries of cloned herpesvirus genomes: mutational analysis of human cytomegalovirus envelope glycoprotein genes. *J. Virol.* 74:7720–7729.
42. Wagner, M., A. Gutermann, J. Podlech, M.J. Reddehase, and U.H. Koszinowski. 2002. Major histocompatibility complex class I allele-specific cooperative and competitive interactions between immune evasion proteins of cytomegalovirus. *J. Exp. Med.* 196:805–816.
43. Atalay, R., A. Zimmermann, M. Wagner, E. Borst, C. Benz, M. Messerle, and H. Hengel. 2002. Identification and expression of human cytomegalovirus transcription units coding for two distinct Fcgamma receptor homologs. *J. Virol.* 76:8596–8608.
44. Messerle, M., I. Crnkovic, W. Hammerschmidt, H. Ziegler, and U.H. Koszinowski. 1997. Cloning and mutagenesis of a herpesvirus genome as an infectious bacterial artificial chromosome. *Proc. Natl. Acad. Sci. USA*. 94:14759–14763.
45. Hengel, H., J.O. Koopmann, T. Flohr, W. Muranyi, E. Goulmy, G.J. Hammerling, U.H. Koszinowski, and F. Momburg. 1997. A viral ER-resident glycoprotein inactivates the MHC-encoded peptide transporter. *Immunity*. 6:623–632.
46. Meyer, T., A. Begitt, I. Lodige, M. van Rossum, and U. Vinkemeier. 2002. Constitutive and IFN-gamma–induced nuclear import of STAT1 proceed through independent pathways. *EMBO J.* 21:344–354.
47. Park, C., M.J. Lecomte, and C. Schindler. 1999. Murine Stat2 is uncharacteristically divergent. *Nucleic Acids Res.* 27:4191–4199.
48. Hengel, H., C. Esslinger, J. Pool, E. Goulmy, and U.H. Koszinowski. 1995. Cytokines restore MHC class I complex formation and control antigen presentation in human cytomegalovirus-infected cells. *J. Gen. Virol.* 76:2987–2997.